ACS APPLIED MATERIALS & INTERFACES

Research Article

www.acsami.org

Innovative Approaches for Converting a Wood Hydrolysate to High-Quality Barrier Coatings

Yingzhi Zhu Ryberg, Ulrica Edlund, and Ann-Christine Albertsson*

Department of Fibre and Polymer Technology, KTH Royal Institute of Technology, SE-10044 Stockholm, Sweden

Supporting Information

ABSTRACT: An advanced approach for the efficient and controllable production of softwood hydrolysate-based coatings with excellent oxygen-barrier performance is presented. An innovative conversion of the spray-drying technique into a coating applicator process allowed for a fast and efficient coating process requiring solely aqueous solutions of softwood hydrolysate, even without additives. Compared to analogous coatings prepared by manual application, the spray-drying produced coatings were more homogeneous and smooth, and they adhered more strongly to the substrate. The addition of glyoxal to the aqueous softwood hydrolysate solutions prior to coating formation allowed for hemicellulose cross-linking, which improved both the mechanical integrity and the oxygen-barrier performance of the coatings. A real-time scanning electron microscopy imaging assessment of the tensile deformation of the coatings allowed for a deeper understanding of the ability of the coating layer itself to withstand stress as well as the coating-to-substrate adhesion.

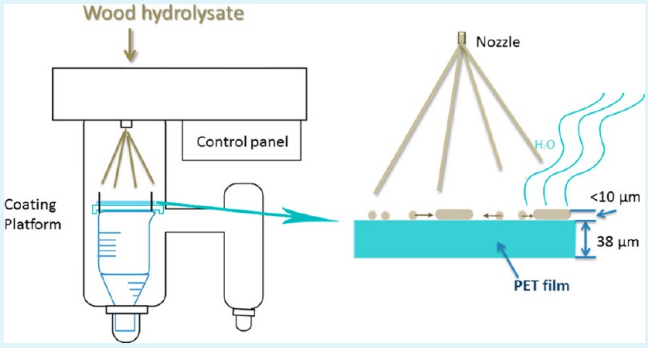

KEYWORDS: *wood hydrolysate, hemicellulose, lignin, spray drying, coatings, real-time SEM, oxygen permeability*

INTRODUCTION

Side streams from the wood processing industry, such as process liquors and wood hydrolysates, are currently being revalued from waste to value-adding side products as their viability as renewable material feedstock is revealed and elaborated.[1,2] There are many approaches to develop valuable products from wood hydrolysates,[3−8] among which a thin barrier layer in a multilayered packaging laminate stands out as a commercially and environmentally attractive application offering an inexpensive and renewable alternative to fossil-based materials[9] with a remarkably good oxygen-barrier performance.[4,10−12] The multilayered packaging laminate composes the barrier as a middle layer, sandwiched between a plastic layer on one side of the middle layer and coated onto a substrate outer layer on the other side, where the barrier layer is to serve as a gas barrier between the middle layer and the first outer layer. The outer layers keep the renewable barrier layer coating (e.g., derived from wood hydrolysate) sealed from the surrounding environment and package contents and provide sufficient mechanical support for future storage and use. Still, to realize this concept and successfully implement any renewable material into a commercial barrier-coating production, a feasible, efficient, scalable, and reproducible processing technique for applying the coating onto a backing substrate is urgently needed.

Much effort has been focused on the fractionation and purification of wood hydrolysates and similar wood-derived process liquors to isolate the main components, hemicelluloses, prior to the production of free-standing films and coatings.[13−15] Such extraction and purification processes are typically expensive and time-consuming. We have proposed an unconventional solution, namely, the utilization of crude wood hydrolysates, and we have demonstrated free-standing films and coatings with a very good barrier performance produced from blends of wood hydrolysates with a second polysaccharide by solution casting.[4,8,16−19] Taking this concept further presents several challenges.

One challenge is in regards to the coating technique. Manual coating on the lab scale is commonly practiced and resembles an industrial roller-coating process. However, quite a low dry content of the coating mixture is typically required to achieve rapid and homogeneous distribution of the liquid-coating mixture on the substrate. As a result, a long drying time is required and hence a long path on the assembly line in a factory. In addition, the thickness and homogeneity of a coating is difficult to control in a manual-coating process. An innovative approach hereby proposed is to convert the spray-drying technique to a coating-layer applicator process. The spray-drying technique is widely used for particles and powder production in the pharmaceutical[20,21] and food industries.[22,23] The spray-drying technique offers efficiency and applicability in large-scale production. In the spray-drying technique, a solution

Received: March 27, 2013
Accepted: August 5, 2013
Published: August 5, 2013

is rapidly transformed into dry particles on the micro scale. The wood hydrolysates are water soluble, which is ideal for a scalable spray-drying technique free from organic solvents. To convert the spray-drying technique from particle to coating production, we designed a platform under the nozzle in the spray dryer and aimed to achieve spray-drying coatings from wood hydrolysates.

Another challenge related to wood hydrolysate coatings is to overcome the inherent brittleness of hemicelluloses, which hampers the mechanical performance of hemicellulose materials in general. It is important that the coatings are ductile enough to endure a certain extent of possible deformation during their manufacture and use. An improvement in ductility may be achieved by plasticization with low molecular weight compounds,[11,24−26] such as glycerol or sorbitol, blending with more ductile macromolecular cocomponents[4,8,16−19] or chemical modification.[11,27] The hemicellulose component of wood hydrolysates have numerous pendant hydroxyl groups available for covalent coupling and thus enables chemical modification that is more stable than physical blending. Clearly, considering the potential application as a middle layer in a multilayered packaging laminate, benign process conditions without toxic solvents/chemicals are required. Dialdehyde induced cross-linking by glyoxal is a promising reaction strategy. Glyoxal is widely used in the paper-coating industry.[28] Previous studies of polysaccharide modification[26,29,30] with glyoxal show that glyoxal reacts with hydroxyl groups to form a cross-linked network.

To improve the mechanical behavior of a wood hydrolysate coating is one challenge, and a quantitative and simultaneously qualitative assessment of the performance is another. The coatings are generally thin and adhere well to the substrate.[4] Conventional tensile testing only provides information on the substrate strength, modulus, and strain and does not reflect the coating properties. To be able to analyze the ductility of the coatings alone, we herein introduce a method allowing for tensile testing under real-time SEM imaging. This provides new insights into the mechanical performance of the wood hydrolysate-based coatings.

Meeting these challenges, our aim was to elaborate and demonstrate an advanced approach to convert a wood process liquor raw material, a wood hydrolysate (WH), into a thin and functional oxygen-barrier coating without additives for the potential application as a middle layer in a multilayered packaging laminate. Our goal was to realize an efficient and reproducible applicator process of the coating-interface layer, to avoid the long drying times hampering manual coating techniques, and to make the coating formulation more cost efficient. We also aimed at decreasing the brittleness of the coatings and improving the substrate adhesion. Here, we propose an innovative conversion of the spray-drying technique to a coating-applicator process in combination with glyoxal treatment of the polysaccharide chains in the WH. In addition, tensile testing under real-time SEM imaging provides new insights into the performance of the WH-based barrier interface.

EXPERIMENTAL SECTION

Wood Hydrolysate (WH). A softwood hydrolysate was generated in a hydrothermal treatment of spruce wood chips in which the chips were heated in an aqueous solution in a liquid-to-wood ratio of 6:1 at 165 °C for 60 min and then for an additional 20 min. The liquid phase was reduced in volume through membrane filtration using a 1 kDa cutoff membrane. The retentate phase was then lyophilized, resulting in a light brown powder herein denoted SW. SW had a low molecular weight (M_w = 2400 g/mol and M_n = 1500 g/mol) and a PDI of 1.9. SW contained mostly oligo- and polysaccharides and 15% lignin. The polysaccharides were chiefly (>90%) the softwood hemicellulose acetylated galactoglucomannan.[19]

Materials. Glyoxal, 40% (w/w) in water solution, was purchased from Sigma-Aldrich (CAS number 107-22-2). It has a density of 1.265 g/mL at 25 °C. Poly(ethylene terephthalate) (PET) films with a thickness of 38 μm were kindly provided by Tetra Pak Packaging Solutions AB and were used as model substrates.

Glyoxal-Mediated SW Cross-Linking. Aqueous solutions (10 g/L) of SW were prepared to which glyoxal was added in the amounts of 0, 5, 10, 20, 35, or 50% (w/w) with respect to SW. The solutions were placed at room temperature on a shaking board moving at a rate of 150 min^{-1}. One solution with 50% (w/w) glyoxal was also prepared at 60 °C. All of these solutions were used for the further production of manual/spray-drying coatings and spray-drying particles.

Coating Production. *Manual Coating.* The SW-based solutions were applied onto PET films with a brush, forming a macroscopically homogeneous and thin liquid layer. The coatings were then air-dried at room temperature for at least 3 h.

Spray-Drying Coating. Spray-drying coatings were produced using a Mini Spray Dryer B-290 (Büchi Labortechnik AG, Switzerland). The SW-based solutions were pumped and heated at 220 °C at the nozzle and then sprayed out as fine droplets into the big chamber. By means of an air flow, the droplets were transported into a small chamber and eventually precipitated into particles in a small vial. A platform was custom-made from customary glass ware for this work and placed in the big chamber under the nozzle for the coating production. The neck of beaker flask was locked in the lower part of the big chamber so that a stable platform was achieved. The PET substrate film was fixed on an aluminum former by staples before being placed on the platform to ensure further the stability of the lightweight films under gas flow during the coating process. The prepared solutions (35−40 mL) were sprayed through the two 0.7 mm fluid nozzles in the spray dryer. The aspirator degree was controlled to be 100%, the inlet temperature, to be over 220 °C, the pump, to be 2−4%, and the gas flow at 30−40 mL/min.

Particles Production. To follow the cross-linking process of the coatings, further structural characterizations with Fourier transform infrared spectroscopy and thermal gravimetric analysis were necessary. For this purpose, microparticles were produced by spray drying from each SW-based solution using the exact same settings as for the coatings production previously explained.

Characterization. *Fourier Transform Infrared (FTIR) Spectroscopy.* FTIR measurements were carried out using a PerkinElmer Spectrum 2000 FTIR with an attenuated total reflectance (ATR) crystal accessory (Golden Gate). The produced SW-based particles were piled above the crystal, and 16 individual scans at 2 cm^{-1} resolution at a range of 4000−600 cm^{-1} were performed for each sample. The background of atmospheric water and carbon dioxide was subtracted automatically. The spectra were analyzed using the Spectrum 5.3 software (PerklinElmer) with baseline corrections and normalizations to allow for comparisons between spectra. Data were further analyzed and plotted in Origin 8.0.

Thermal Gravimetric Analysis (TGA). TGA was performed on a Mettler Toledo TGA/DSC 851 instrument. The particles were placed in a ceramic cup in amounts of 7−9 mg. The samples were heated from 30 to 600 °C at 10 °C/min under a nitrogen flow (50 mL/min). The data was collected by Mettler-STARe Evaluation software and further plotted by Origin 8.0.

Scanning Electron Microscopy (SEM). A table-top SEM, Hitachi TM1000, was used to analyze the surface of the coatings at an accelerating voltage of 15 kV. A charge-up reduction mode was chosen during the observation. The surfaces of the coatings were examined at magnifications of 500× and 1000×.

Micromechanical Tensile Testing with Integrated SEM. A table-top SEM, Hitachi TM1000, was used together with a Deben Microtest, a small tensile test device allowing for the real-time observation of the

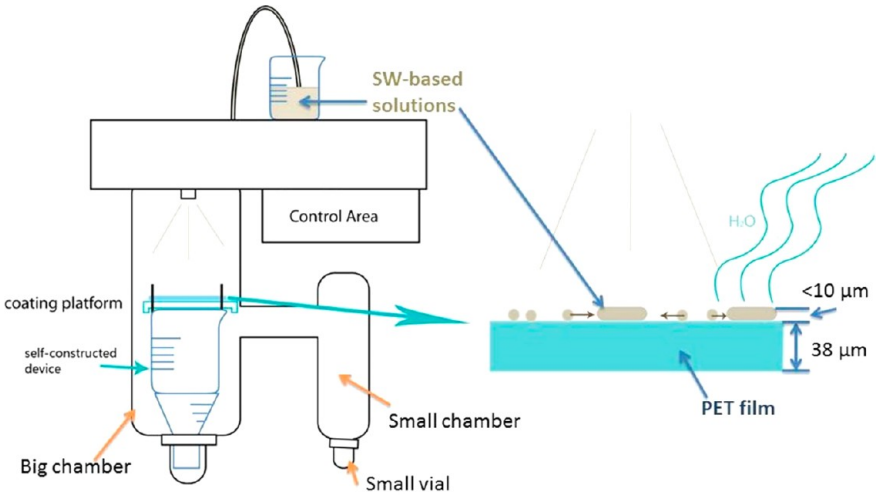

Figure 1. Schematic illustration of a spray dryer with a custom-made coating platform on the left and the mechanism of coating process on the right.

surface of the coatings under a controlled pulling process. The Deben Microtest device was small enough to be placed in the chamber under the SEM electronic beam so that the imaging and tensile-stretching process could progress simultaneously.

The SW-based coatings were cut into rectangular specimens with a width of 5 mm. The coatings were mounted into the Deben Microtest device with a gauge length of 10 mm and load cell of 200 N. The coatings were first observed by microscopy at a magnification of 30×, and the position of each coating was adjusted so that the image was in a perpendicular position. The microtensile test device was activated with a pulling speed of 1 mm/min. The images were sampled starting from an elongation of 1.0 mm and every 0.5 mm until a complete sample break was recorded. The position of the coating was adjusted at the same time to ensure that the same region was observed all the time.

Oxygen Permeability (OP). Oxygen permeability was measured with a Mocon 220. The coatings were preconditioned at 50 and 80% relative humidity (RH) and room temperature. They were then cut into square-shaped specimens and sandwiched individually between two aluminum foils with a round opening (5 cm^2). The humidity was set at 50%, and the mode for testing was converging by more than eight cycles. At least two individual samples were measured for each SW-based coating.

RESULTS AND DISCUSSION

We aimed to develop an approach to apply a wood hydrolysate (WH), a process liquor-derived biomass, as a coating layer. The core concept is to derive such a coating with the appropriate properties to serve as a oxygen-barrier layer. This barrier may then be sandwiched in between an outer protective plastic layer and a substrate backing layer and hence constitute the middle layer in a multilayered packaging laminate. Thus, in a possible potential application, the wood hydrolysate layer will be sealed inside the laminate, just like in many commercial food packaging laminates, and not directly exposed to the atmosphere or moisture or subjected to direct mechanical wear. Still, in the development process, it will provide useful information to consider the direct influence of the environment, for example, the sensitivity to the surrounding relative humidity. Accordingly, in this work, surface coatings of WH on a substrate are developed and studied without further lamination. The WH used was a softwood hydrolysate (SW) produced during a hydrothermal treatment of spruce wood chips. It contained 15% lignin and a large amount of hemicelluloses of the acetylated galactoglucomannan type (AcGGM). PET was used herein as a model substrate because it is commonly used in packaging. In addition, PET is a commonly applied model substrate in the food packaging industry, providing a smooth surface ideal for elaborating coating mixtures and a viable coating process.

Previously, we have demonstrated a strategy in which excellent oxygen-barrier coatings from blends of WH and a renewable cocomponent were produced by a manual coating technique.[4,8,16−19] The blending process produced homogeneous coatings on PET but introduced a significant amount of a cocomponent that was neither cost-effective nor practical for industrial implementation. In addition, manual coating required long drying times. Herein, we propose a creative and efficient coating technique, converted spray-drying coating.

Coating by a Converted Spray-Drying Technique. A spray dryer customarily used for particles production was redesigned to allow efficient coating production of SW-based formulations onto PET substrates. A steady platform was built and placed under the nozzle in the big chamber of the spray dryer (Figure 1), and the PET film was fixed on the platform. During the coating process, the SW-based solutions were pumped to the nozzle, heated at 220 °C, and sprayed out as droplets into the big chamber. The droplets hit the PET films with a high speed and dried rapidly assisted by a steady air flow. SW droplets thus formed a homogeneous coating firmly attached to the substrate. The temperature at the nozzle position is the inlet temperature (T_{inlet}) and was controlled to be around 220 °C. The solution is only in contact with this high temperature for a very brief time. The solution is then immediately transformed into small droplets and transferred as a mist to the big chamber. The so-called outlet temperature (T_{outlet}), the temperature recorded at the outlet from the big chamber to the small chamber (Figure 1), was in the range of 100−110 °C for all experiments, resulting in a big-chamber temperature gradient from 100 to 220 °C. In this temperature range and combined with a constant air flow, water and any traces of unreacted glyoxal rapidly evaporate before the droplets hit the substrate on the coating platform during the spray drying. The boiling temperature for a 40% aqueous solution of glyoxal is 104 °C.

The coatings were prepared from aqueous solutions of SW (10 g/L) both manually and by spray-drying coating for comparison. Spray-drying coating was much more efficient than

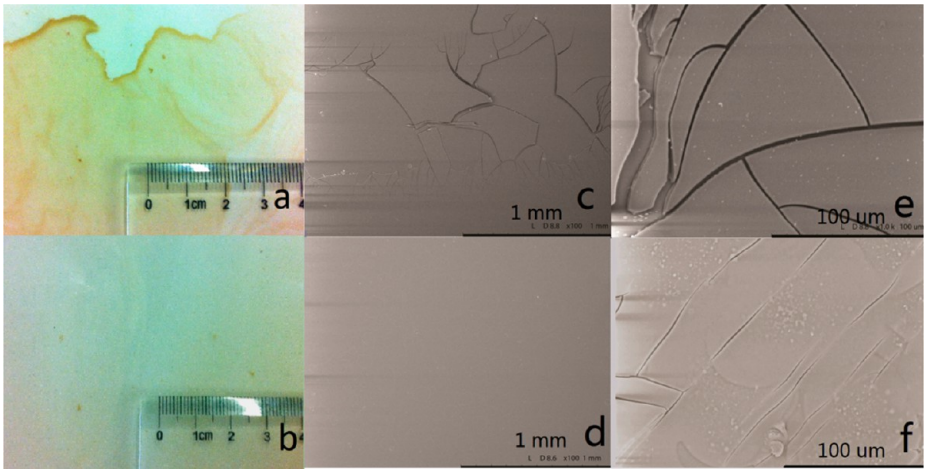

Figure 2. Images of SW coatings on PET. (a) Manually coated and (b) spray-drying coated. SEM micrographs of SW coatings on PET produced (c, e) manually and (d, f) by the spray-drying technique at magnifications of (c, d) 100× and (e, f) 1000×.

manual coating, requiring less than 5 min for completion, whereas 3 to 5 h was needed in the case of manual coating. The thickness of a coating made by the spray-drying technique can be readily finely tuned by varying the amount of spray solutions.

The coating topographies are shown in Figure 2a,b. The spray-drying coated films were much more homogeneous than manually coated ones. During manual coating, SW-based solutions spread unevenly on PET substrate, whereas the droplets separated evenly by an air flow during spray-drying coating, making the resulting coatings much more homogeneous in the latter case. The spray-drying technique produced coatings that were also microscopically more homogeneous. Even at low magnification, cracks appeared on the surface of manually produced coatings in contrast to the spray-drying coatings (Figure 2c,d). At higher magnification, SEM images reveal that the cracks in the coatings produced manually were interconnected and that the adhesion to the substrate was insufficient (Figure 2f). The spray-drying technique produced coatings that fully covered the substrate surface and displayed small cracks and some particles (Figure 2f). The superior substrate attachment achieved by spray-drying coating is important from a barrier property perspective. The oxygen permeability (OP) is a key parameter in the intended application and is quantified as the volume of oxygen passing over time through a film of a given area and thickness at a given humidity and pressure. In food packaging applications, a value of 38.9 μm cm^3 m^{-2} day^{-1} kPa^{-1} is considered a good barrier.[31,32] Both spray drying and manually produced coatings improved the OP of the substrate PET film, having an OP of 14.6 μm cm^3 m^{-2} day^{-1} kPa^{-1} in the uncoated state at 50% relative humidity (RH). Manually produced SW coatings showed a reduced OP to 10.0 μm cm^3 m^{-2} day^{-1} kPa^{-1}, whereas the analogous coating produced by the spray-drying technique reduced OP to 8.1 μm cm^3 m^{-2} day^{-1} kPa^{-1}. SW-based coatings are hence competitive with many synthetic conventional packaging polymers. For instance, high-density polyethylene (HDPE) has an OP in the range of 390−780 μm cm^3 m^{-2} day^{-1} kPa^{-1} and polypropylene (PP), 580−970 μm cm^3 m^{-2} day^{-1} kPa^{-1}.[33] The well-known gas barrier ethylene vinyl alcohol (EVOH) has OP values from 0.1 to 12 μm cm^3 m^{-2} day^{-1} kPa^{-1} in the range of 0 to 95% RH.[34]

The spray-drying coating approach improved the production efficiency, the coating appearance, and the performance of the coatings. However, some cracks still appeared in the coatings (Figure 2f), which are probably due to the brittle nature of hemicelluloses being the major component of wood hydrolysates in general and the SW used here in particular.[3,28] AcGGM is a polysaccharide with plentiful OH groups and intra- and intermolecular hydrogen-bond interactions, which, together with the strong interactions between lignin and hemicellulose, contribute to the formation of a densely packed solid matrix as proposed and discussed by a calculation model in our previous studies.[16−18] The densely packed morphology plays an integral role in the oxygen-barrier performance, but at the same time it restrains molecular mobility in the matrix of the SW and leads to a rigid and brittle coating. Even though the spray-drying technique produced coatings that were well adhered to the PET substrate, some cracks were unavoidable. To develop further the approach and to tune the coating performance, the chains in SW were chemically modified, aiming to suppress cracking and at the same time improve the barrier and tensile performance of the coatings.

Coating Performance Improvement by Glyoxal Treatment of SW. Numerous hydroxyl groups on the backbones of the AcGGM component of SW offer many potential sites for chemical modification. The challenge is to develop green and benign process conditions under which the reaction will still proceed efficiently and at high yield. Glyoxal coupling offers the chemistry that we seek, because it is water soluble and efficient in its reaction with hydroxyl functionalities on polysaccharide backbones.[26,30] Glyoxal treatments are industrially used for starch-based formulations and cellulose derivaties (e.g., in paper and textile sizing).[28]

A series of aqueous solutions of glyoxal and SW were prepared, with glyoxal in the amounts of 0, 5, 10, 20, 35, and 50% (w/w) of the mass of SW, respectively. The samples were labeled according to the following

$$\mathrm{s/m} - \mathrm{SW} - x\mathrm{G}$$

where s/m denotes either spray-drying coating (s) or manual coating (m). xG means that x% of glyoxal was added and is omitted for the reference samples where no glyoxal was added.

Glyoxal-treated SW solutions were used for the production of coatings on PET using both the converted spray-drying

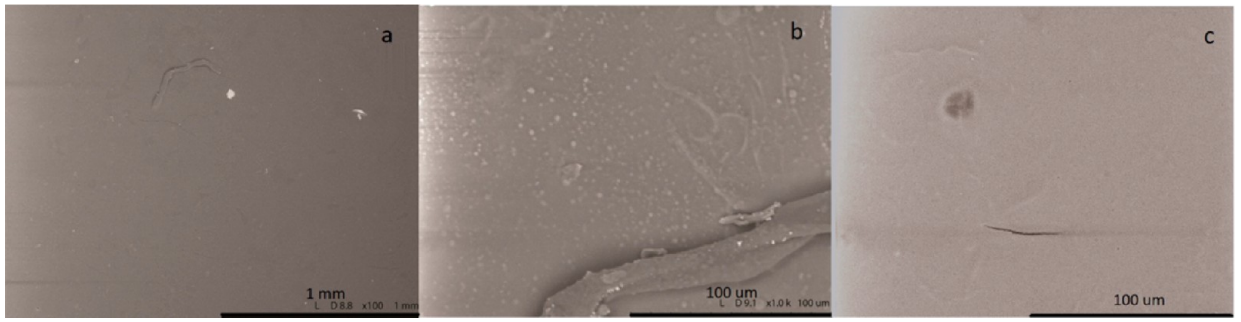

Figure 3. SEM micrographs of s-SW-50G coatings at magnifications of (a) 100× and (b, c) 1000×.

process and manual application. Macroscopically, the spray-drying technique produced coatings that appear identical whether glyoxal was added to the SW solution or not, indicating that the spray-drying technique was reproducible. The topography of s-SW-50G was further observed by SEM (Figure 3) and compared to the coating analogously prepared without the addition of glyoxal, s-SW. The cracks were small and scarce, and the surface of s-SW-50G was more coherent and intact compared to s-SW.

Appropriate mechanical integrity is important for packaging laminates. PET serves as a robust substrate offering sufficient mechanical support as a substrate. However, the mechanical intergrity of the coating layer is also of importance considering that each individual crack impairs the oxygen-barrier performance. Avoiding or minimizing crack formation and propagation during the manufacture of packaging products is thus an important driver for the glyoxal treatment of SW-coating formulations. Observing the coatings' deformation under the course of action would provide deaper insights into their mechanical response and interaction with the substrate. To realize this, a microtensile test device exerting a controlled pulling process was used inside the vacumm chamber of an SEM microscope to allow for the real-time observation of sample tensile behavior under load until break (schematically illustrated in Figure S1, Supporting Information). The coatings were placed with the coated side up and aligned to ensure that pulling was performed in a direction perpendicular to the camera. The coated substrates were then subjected to tensile deformation at a controlled speed and load during which a real-time strain-stress curve was generated and images were recorded simultaneously. The instrument set up allows the measurement to be paused at a desired elongation rate or time for additional image capture. The original length of the coated samples were 10 mm. The images were captured at elongations of 1.0, 1.5, 2.0, 2.5, 3.0, and 3.5 mm. Sample breaks were usually recorded around 3.5 mm.

Both manually produced and spray-drying-technique produced coatings without glyoxal treatment (m-SW and s-SW, respectively) were subjected to real-time SEM, and the progressing tensile deformations are shown in Figure 4. The many cracks initially present on the m-SW coating surface propagated, and the coating started to split into debris even at low strain (Figure 4a). With increasing strain, many small square-shaped pieces appeared all over the surface as the brittle coating started to detach from the substrate and split into fine particles. The s-SW coating showed minor initial cracking and some circular patterns, the latter originating from the individual droplets settling on the substrate in the spray-drying coating process. As mentioned previously, the fine droplets of sample solutions were formed in the nozzle and transferred by spraying into the big chamber where they landed on the substrate surface. The temperature in the big chamber was between 100 and 220 °C and combined with the continuous airflow, the droplets dried quickly and the ability of coalescence was reduced, creating remaining traces of circular patterns shown in Figure 4b. During the elongation, new cracks formed and propagated and square-shaped debris started to form on the surface, but the substrate adhesion was intact until the end of the pulling process at 3.5 mm of elongation (Figure 4b). All in all, the mechanical integrity and substrate adhesion was superior for the coatings prepared by spray drying compared to those produced manually.

The s-SW-50G coatings (Figure 4c) initially had a smoother and more coherent surface compared with m-SW and s-SW. During the course of elongation, some cracks formed and propagated in the direction of the tensile pulling direction in a proportion similar to that observed for the s-SW coating. The debris formation was much less expressed for s-SW-50G than for either m-SW and s-SW, and a larger extent of expanding and pulling was possible. The deformation of the coating layer coincided with the PET substrate deformation. The glyoxal treatment hence resulted in an improvement of the ductility of the SW coatings.

The SW coatings were further assessed with respect to their oxygen permeability at 50% RH (Table 1) to reveal their potential function as a barrier layer in packaging applications. All SW coatings improved the oxygen-barrier ability of the PET substrate. Spray drying produced coatings that generally improved the barrier performance more than the manual coatings of analogous compositions, which is reasonable considering the more homogeneous and complete coverage achieved in the spray-drying process as compared to manual coating, as verified by SEM analysis and discussed previously.

With increasing glyoxal amounts, the OP value generally decreased from 8.1 (s-SW) to 1.6 μm cm^3 m^{-2} day^{-1} kPa^{-1} (s-SW-50G). Compared with previously reported coatings based on blends of a softwood hydrolysate having an OP of 1.6 μm cm^3 m^{-2} day^{-1} kPa^{-1} (wood hydrolysate/carboxyl methyl cellulose (CMC) 1:1) and 8.9 μm cm^3 m^{-2} day^{-1} kPa^{-1} (wood hydrolysate/chitosan 1:1),[4,16] respectively, the new approach in this work gave competitive OP results in a much more efficient and reproducible process, and it is noteworthy that it did so without any macromolecular additives. Neither were conventional plasticizers like glycerol or sorbitol, often used for similar polysaccharide based films, necessary. The coatings prepared with this new approach were also competitive with the xylan-rich wood hydrolysate coatings prepared from hardwood hydrolysates mixed with mineral additives such as montmor-

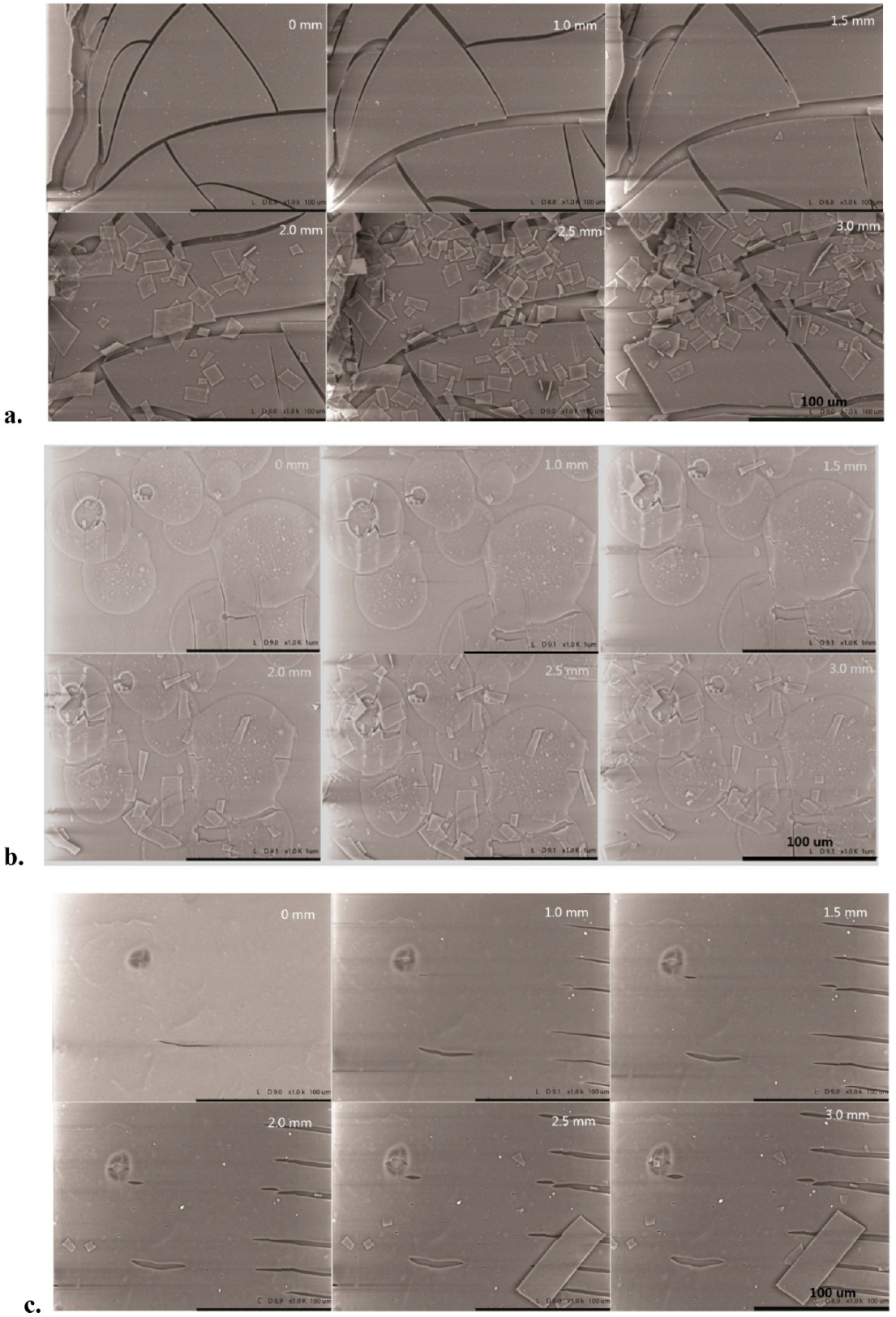

Figure 4. Real-time SEM micrographs of SW-based coatings captured during tensile deformation in a perpendicular direction. The images were frozen at elongations of 0, 1, 1.5, 2, 2.5, and 3 mm. (a) m-SW, (b) s-SW, and (c) s-SW-50G.

illonite clay.[8] In a food packaging application, a low OP is a prerequisite to extend the shelf life of the contained food stuff. Hemicelluloses are known for providing good oxygen barriers.[10−12,16−19,22−24] For instance, purified arabinoxylan plasticized with 40% sorbitol was reported to have an OP value of 4.7 μm cm^3 m^{-2} day^{-1} kPa^{-1}.[24] Commercial and commonly used packaging plastics such as PP and HDPE typically have high permeability values, above 300 μm cm^3 m^{-2} day^{-1} kPa^{-1}.[33]

dx.doi.org/10.1021/am401102h | ACS Appl. Mater. Interfaces 2013, 5, 7748−7757

Table 1. Oxygen Transition Rate (OTR) and Oxygen Permeability (OP) Values at 50 and 80% RH for SW-Based Coatings

coatings on PET	thickness (μm)	OTR at 50% RH ($cm^3\ m^{-2}\ day^{-1}$)	OP at 50% RH ($\mu m\ cm^3\ m^{-2}\ day^{-1}\ kPa^{-1}$)	OP at 80% RH ($\mu m\ cm^3\ m^{-2}\ day^{-1}\ kPa^{-1}$)
	38.0	38.9	14.6	15.7
m-SW	39.0 ± 0.8	26.1 ± 0.5	10.0	
m-SW-50G	40.4 ± 1.2	19.2 ± 1.8	7.7	
s-SW	40.4 ± 1.8	20.4 ± 4.6	8.1	12.0
s-SW-5G	39.1 ± 1.1	20.0 ± 7.8	7.7	
s-SW-10G	40.1 ± 0.9	17.5 ± 2.2	6.9	
s-SW-20G	42.7 ± 3.0	13.8 ± 3.9	5.8	
s-SW-35G	39.4 ± 0.5	7.25 ± 0.6	2.8	
s-SW-50G	46 ± 3.4	3.6 ± 1.1	1.6	1.3

Scheme 1. Schematic Illustration of Plausible Reaction Pathways of AcGGM in the Presence of Glyoxal in Aqueous Solution[a]

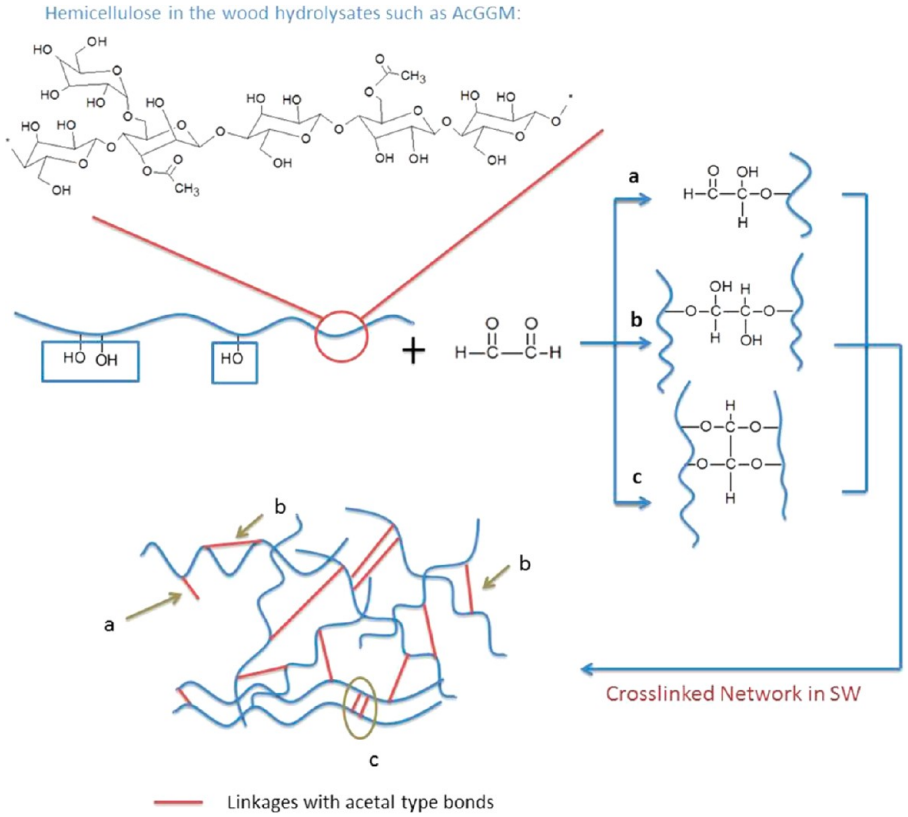

[a]The resulting cross-linked network may contain several different types of linkages. Glyoxal can react with (a) one or (b) two hydroxyl groups and form hemi-acetal bonds, whereas a coupling with (c) two or more hydroxyl groups may form an acetal linkage.

PVC has a lower OP (20−80 $\mu m\ cm^3\ m^{-2}\ day^{-1}\ kPa^{-1}$), as does PET (12−16 $\mu m\ cm^3\ m^{-3}\ day^{-1}\ kPa^{-1}$).[33] Polylactide, often studied as a renewable packaging plastic alternative, has quite high OP values (~600 $\mu m\ cm^3\ m^{-2}\ day^{-1}\ kPa^{-1}$).[6] The wood hydrolysate coatings presented herein are hence well competitive with the commercial packaging materials in terms of their oxygen-barrier performance. EVOH is considered as a very good barrier at 0% RH, with an OP as low as 0.3 $\mu m\ cm^3\ m^{-2}\ day^{-1}\ kPa^{-1}$, although the OP increases up to 12 $\mu m\ cm^3\ m^{-2}\ day^{-1}\ kPa^{-1}$ at 99% RH.[34]

The relative humidity is strongly affecting the oxygen-barrier performance of hydrophilic materials, as evident for EVOH, and is expected to influence also the wood hydrolysate coatings given their high content of polysaccharides. Yet, it has been shown that a nonhighly purified wood hydrolysate may perform better in terms providing a good oxygen barrier than analogous formulations on the basis of highly refined hemicellulose.[16−18]

To elaborate the ability of these wood hydrolysate coatings to perform under high-humidity conditions, the OP for the PET substrate alone, s-SW, and s-SW-50G were assessed at 80% RH. As shown in Table 1, the OP of PET increased only slightly from its value at 50% RH to 15.7 $\mu m\ cm^3\ m^{-2}\ day^{-1}\ kPa^{-1}$ at 80% RH. When PET was coated with s-SW, the OP improved as compared to pristine PET (12.0 $\mu m\ cm^3\ m^{-2}\ day^{-1}\ kPa^{-1}$) but less so at 80% RH than at 50% RH. Remarkable for a polysaccharide-based material, s-SW-50G maintained its excellent oxygen-barrier performance even at 80% RH. The glyoxal treatment hence effectively created a network structure that withstands its stability at high-RH conditions. The structure was stable and maintained its stability to moisture over the time span of 4 days that was required for conditioning and measurement at 80% RH, indicating that the network is mainly composed of stable acetal bonds rather than reversible hemiacetal linkages, as discussed in the following section. The

network formation hence improved not only the mechanical performance and appearance of the coating but also the moisture resistance of the wood hydrolysate and raises the need and the interest to further explore, from a chemical perspective, why and how glyoxal dramatically improves the quality of wood hydrolysate coatings.

Chemical Perspective on Glyoxal Treatment. The glyoxal treatment effect on the SW-based-coatings performance can be understood by elucidating the chemical modification affected on the hemicellulose component of the SW. Several routes are possible for the reaction between the aldehyde carbonyl groups of glyoxal with the hydroxyl pendant groups of the AcGGM component in the SW (Scheme 1). Depending on the number of hydroxyl groups involved in the coupling reaction, either a hemiacetal or an acetal may form. At low molar ratios of glyoxal, such as in s-SW-5G, a reaction pathway involving only one hydroxyl group is more likely, resulting in the formation of modified pendant groups (Scheme 1, reaction pathway a). Higher molar ratios of glyoxal enhance the production of intra- and intermolecular cross-links by hemiacetal (Scheme 1, reaction pathway b) and acetal (Scheme 1, reaction pathway c) formation. In the former situation, a network is not efficiently formed, and the produced hemiacetal/acetal bonds may even disturb the original molecular order in the SW with extensive hydrogen-bond interactions. This could explain why s-SW-5G showed only a minor improvement in OP compared with s-SW (Table 1). With increasing amounts of glyoxal, a network was more extensively formed, providing a more efficient obstruction to oxygen diffusion through the matrix that in turn lowered the OP. The formation of a network structure also contributes to an increase in the mechanical integrity, as observed for glyoxal treated coatings (Figure 4).

To allow for the analysis of the chemical structures produced in the reaction of SW with glyoxal, microparticles with identical compositions as those of the coatings were produced by the spray-drying technique. The Fourier transform infrared (FTIR) spectroscopy results of SW-based particles with various amounts of glyoxal are shown in Figure 5 and reveal a trend that is consistent with the suggested cross-linking mechanism discussed previously. With the increasing amount of glyoxal, gradual changes are apparent in the FTIR spectra in three particular wavenumber regions at around 1240, 1732, and 3350 cm^{-1} (highlighted in the insets of Figure 5). The band at 1240 cm^{-1} is attributed to the C−O−C vibration and bending,[35] and with the increasing amount of glyoxal, this peak gradually decreased and is shifted into a higher wavenumber. The C−O−C bonds are abundant in the hemicellulose component of SW and are affected by the formation of hemiactal/acetal bonds glyoxal coupling. The band at 1730 cm^{-1} is a typical carbonyl peak, and it followed the same trend as the band at 1240 cm^{-1}. AcGGM in SW is acetylated, explaining the presence of this band in all formulations. Nonreacted glyoxal contain carbonyl functionalities as well, so the fact that the carbonyl band intensity decreases with the increasing amount of glyoxal in the SW matrix indicates that glyoxal reacted to a very high yield, converting the carbonyls to hemiacetal and acetal groups instead. The broad band at 3350 cm^{-1} represents OH group stretching. This band is typically broad instead of a well-resolved peak because of the extensive hydrogen-bonding interactions between the hydroxyl groups. With increasing amounts of glyoxal, the OH bands generally shifted slightly to a lower wavenumber and also to a higher intensity, which indicates an increasing presence of OH groups and hydrogen-bond interactions. Noteworthy, SW-5G was an exception to this trend, showing a stronger shift in the OH band than SW-10G. This is in agreement with the suggested reaction pathways at low and moderate glyoxal molar ratios, respectively. In the former case, more pendant groups and intramolecular hemiacetal bonds were formed, which accordingly introduced more hydroxyl groups in the material.

TGA analysis results sustain the FTIR and OP results (Figure 6). A main thermal transition can be observed in the thermogram of SW-0G at 305.0 °C. This transition shifted up to 310.5 °C with increasing amounts of glyoxal, indicating that SW became more thermally stable with the build up of a cross-linked network. A new transition appeared at 192 °C. This transition became more pronounced and shifted to higher temperatures (to 202 °C for SW-50G) with increasing glyoxal

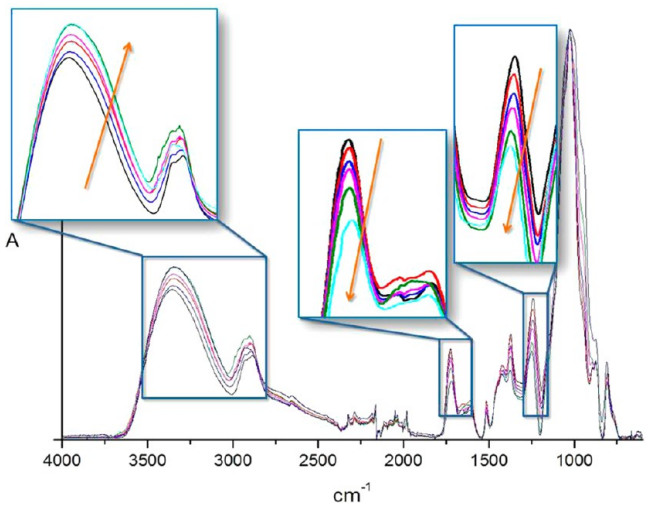

Figure 5. FTIR spectra of microparticles produced by the spray-drying technique from aqueous solutions of SW and 0, 5, 10, 20, 35, or 50% (w/w) glyoxal. The arrows indicate the trend with increasing amounts of glyoxal.

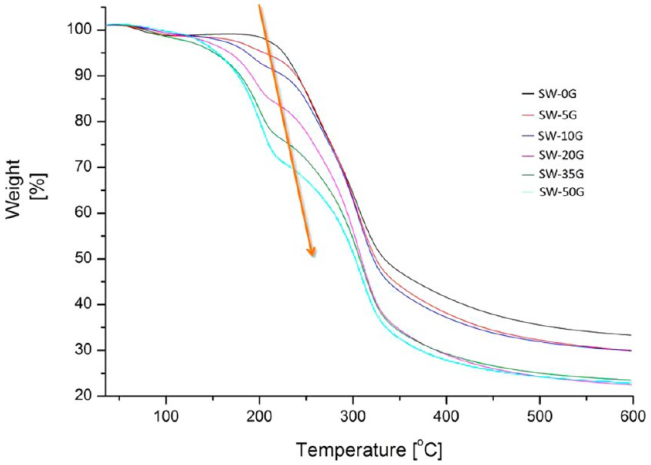

Figure 6. TGA thermograms of microparticles produced by the spray-drying technique from aqueous solutions of SW and 0, 5, 10, 20, 35, or 50% (w/w) glyoxal. The arrow shows the trend with increasing amounts of glyoxal.

dx.doi.org/10.1021/am401102h | ACS Appl. Mater. Interfaces 2013, 5, 7748−7757

amounts, which may be attributed to the formation of hemiacetal bonds that formed tails and intramolecular bonds. (Scheme 1, reaction pathways a and b)

Potential Effects of the Glyoxal Treatment of the Coatings. Glyoxal in larger amounts is a potential human health risk, so it is important to control the amount of possible free glyoxal in packaging materials. In the current work, the wood hydrolysate coatings are developed to serve as the middle layer in the multilayered packaging laminate. The plastic laminate outer layer covering the wood hydrolysate coatings can be designed to provide a good barrier for the migration of glyoxal. However, it is still important to know the amount of free glyoxal, if any, in the barrier layer to take appropriate action in a potential application.

There are two main concerns. First, there are possibly unreacted glyoxal residues in the coatings. Second, the hemiacetal bonds formation may be partly reversible at high relative humidities or water contents. Hemiacetal cleavage would lead to the reformation of free glyoxal in the coating. As discussed previously, both hemiacetal and acetal bond formation may occur in the cross-linking reaction, and to minimize the potential extent of glyoxal formation resulting from hemiacetal cleavage, it is important to form stable acetal bonds in the coatings.

For the glyoxal-treated SW coatings, the TGA and FTIR results show that the amount of free glyoxal in the coatings is very low, if any. The anhydrate state of glyoxal has a boiling temperature at 50.4 °C, whereas the corresponding temperature for the 40% aqueous solution is 104 °C. TGA thermograms show no detectable weight loss for any of the SW coating samples at 104 °C. There were very small weight losses (<5%). A small weight loss of about 4% before 100 °C was detected for SW-0 (not glyoxal treated), but this decreased to less than 2% for glyoxal treated samples. This indicates that the small weight loss before 100 °C was probably due to the evaporation of water and was not due to residual glyoxal. As discussed previously, FTIR analyses showed that carbonyl groups decreased, whereas glyoxal contents increased, which is quite the opposite of what would be detected if free glyoxal were present in the samples. These results are reasonable considering the spray-drying coating production parameter settings. The chamber temperature was between 100 to 220 °C, which is above the boiling point for water and free glyoxal. After the reacted and conditioned glyoxal-treated wood hydrolysate was pumped to the nozzle, the water and unreacted glyoxal was quickly removed, and the network structure was fixed in the wood hydrolysate. With very little residual water present in the coatings, this network will be stable. The low water content also inhibits the possible reverse reactions of hemiacetal linkages. Regarding the ratio of stable acetal bonds to hemiacetal bonds in the treated SW coatings, the much improved moisture sensitivity and the very low OP at 80% RH strongly indicate there was a large amount of stable acetal bonds in s-SW-50G, which was sufficient to preserve the oxygen-barrier performance even at high RH.

The glyoxal treatment effectively introduced a modification of the hemicellulose component of the SW that mediated an improvement in the ability of the material to withstand tensile stress, moisture, and the diffusion of oxygen through the matrix. All of these properties are important for a barrier material, and the increase the potential of SW-based coatings to replace convention barrier layers in multilayered packaging solutions.

CONCLUSIONS

The challenges of producing a homogeneous and functional barrier coating from a hemicellulose-rich and lignin-containing biomass were met by developing a spray-drying-based processing strategy in combination with a chemical modification in aqueous solution. The biomass was a softwood hydrolysate (SW), an aqueous process liquor derived from the hydrothermal treatment of spruce. The spray-drying technique produced coatings, 1−5 μm thick, that were macroscopically and microscopically more homogeneous than the manually produced ones and were superior in terms of their oxygen-barrier properties and substrate adhesion. The process allowed for the utilization of the SW without any additives as well as the use of the biomass raw material without extensive purification. Further improvement of the wood hydrolysate-coating performance was achieved by glyoxal modification in aqueous solution at ambient temperature prior to spray drying. Glyoxal treatment affords cross-linking of the hemicellulose component of the SW via the production of intra- and intermolecular cross-links by hemiacetal and acetal coupling. Manually produced SW coatings had an oxygen permeability (OP) of 10.0 μm cm^3 m^{-2} day^{-1} kPa^{-1}, whereas the analogous coating produced by the spray-drying technique reduced the OP value to 8.1 μm cm^3 m^{-2} day^{-1} kPa^{-1} and glyoxal-treated SW coatings had OP values as low as 1.6 μm cm^3 m^{-2} day^{-1} kPa^{-1}. The addition of glyoxal also improved the resistance to moisture of SW, and a remarkably low OP (1.3 μm cm^3 m^{-2} day^{-1} kPa^{-1}) was displayed by a glyoxal-treated SW coating at a relative humidity as high as 80%. The tensile behavior of the coating itself was assessed by a microtensile testing set up, allowing for the real-time SEM imaging of the load applied tensile deformation until break. Spray-drying coating adhered better to the substrate, and additional glyoxal treatment contributed further to an increase in the mechanical integrity. Renewable oxygen-barrier materials may serve as the middle barrier layer in a multilayered packaging laminate.

ASSOCIATED CONTENT

Supporting Information

Deformation process of the SW-50G coating under tensile testing captured by real-time SEM imaging and a schematic illustration of the real-time SEM device for tensile testing. This material is available free of charge via the Internet at http://pubs.acs.org.

AUTHOR INFORMATION

Corresponding Author

*Tel. +46-8-790 82 74. Fax: +46-8-20 84 77. E-mail: aila@kth.se

Notes

The authors declare no competing financial interest.

ACKNOWLEDGMENTS

The authors gratefully thank VINNOVA (project no. 2009-04311) for financial support, Södra Innovation for kindly providing the softwood chips, and Tetra Pak Packaging Solutions for providing the PET films.

REFERENCES

(1) Ragauskas, A. J.; Williams, C. K.; Davison, B. H.; Britovsek, G.; Cairney, J.; Eckert, C. A.; Frederick, W. J.; Hallett, J. P.; Leak, D. J.;

Liotta, C. L.; Mielenz, J. R.; Murphy, R.; Templer, R.; Tschaplinski, T. *Science* **2006**, *311*, 484−489.
(2) Dahlman, O.; Edlund, U.; Albertsson, A.-C.; Lindblad, M. S.; Parkaas, J. *Utilization of a Wood Hydrolysate*. Patent EP 2067793/WO 2009068525 A1, 2009.
(3) Hansen, N. M. L.; Plackett, D. *Biomacromolecules* **2008**, *9*, 1493−1505.
(4) Edlund, U.; Ryberg, Y. Z.; Albertsson, A.-C. *Biomacromolecules* **2010**, *11*, 2532−2538.
(5) Albertsson, A.-C.; Voepel, J.; Edlund, U.; Dahlman, O.; Söderqvist-Lindblad, M. *Biomacromolecules* **2010**, *11*, 1406−1411.
(6) Saadatmand, S.; Edlund, U.; Albertsson, A.-C. *Polymer* **2011**, *52*, 4648−4655.
(7) Steen, E. J.; Kang, Y.; Bokinsky, G.; Hu, Z.; Schirmer, A.; McClure, A.; del Cardayre, S. B.; Keasling, J. D. *Nature* **2010**, *463*, 559−562.
(8) Yaich, A. I.; Edlund, U.; Albertsson, A.-C. *Carbohydr. Polym.* **2012**, DOI: 10.1016/j.carbpol.2012.10.079.
(9) Siracusa, V.; Rocculi, P.; Romani, S.; Rosa, M. D. *Trends Food Sci. Technol.* **2008**, *19*, 634−643.
(10) Hartman, J.; Albertsson, A. C.; Sjöberg, J. *Biomacromolecules* **2006**, *7*, 1983−1989.
(11) Hartman, J.; Albertsson, A.-C.; Lindblad, M. S.; Sjöberg, J. *J. Appl. Polym. Sci.* **2006**, *100*, 2985−2991.
(12) Mikkonen, K. S.; Heikkilä, M. I.; Helén, H.; Hyvönen, L.; Tenkanen, M. *Carbohydr. Polym.* **2010**, *79*, 1107−1112.
(13) Fundador, N. G. V.; Enomoto-Rogers, Y.; Takemura, A.; Iwata, T. *Carbohydr. Polym.* **2012**, *87*, 170−176.
(14) Pinto, P. C.; Evtuguin, D. V.; Neto, C. P. *Carbohydr. Polym.* **2005**, *60*, 489−497.
(15) Teleman, A.; Tenkanen, M.; Jacobs, A.; Dahlman, O. *Carbohydr. Res.* **2002**, *337*, 373−377.
(16) Zhu Ryberg, Y. Z.; Edlund, U.; Albertsson, A. C. *Biomacromolecules* **2011**, *12*, 1355−1362.
(17) Zhu Ryberg, Y. Z.; Edlund, U.; Albertsson, A. C. *Biomacromolecules* **2012**, *13*, 2570−2577.
(18) Ibn Yaich, A.; Edlund, U.; Albertsson, A.-C. *Biomacromolecules* **2011**, *13*, 466−473.
(19) Saadatmand, S.; Edlund, U.; Albertsson, A.-C.; Danielsson, S.; Dahlman, O. *Environ. Sci. Technol.* **2012**, *46*, 8389−8396.
(20) Mehnert, W.; Mäder, K. *Adv. Drug Delivery Rev.* **2001**, *47*, 165−196.
(21) Ré, M.-I. *Drying Technol.* **2006**, *24*, 433−446.
(22) Gibbs, B. F.; Kermasha, S.; Alli, I.; Mulligan, C. N. *Int. J. Food Sci. Nutr.* **1999**, *50*, 213−224.
(23) King, A. H. In *Encapsulation and Controlled Release of Food Ingredients*; Risch, S. J., Reineccius, G. A., Eds.; American Chemical Society: Washington, DC, 1995; Vol. *590*, pp 26−39.
(24) Mikkonen, K. S.; Heikkinen, S.; Soovre, A.; Peura, M.; Serimaa, R.; Talja, R. A.; Helen, H.; Hyvonen, L.; Tenkanen, M. *J. Appl. Polym. Sci.* **2009**, *114*, 457−466.
(25) Gröndahl, M.; Eriksson, L.; Gatenholm, P. *Biomacromolecules* **2004**, *5*, 1528−1535.
(26) Mikkonen, K. S.; Heikkilä, M. I.; Willför, S. M.; Tenkanen, M. *Int. J. Polym. Sci.* **2012**, 482810-1−482810-8.
(27) Kelley, S. S.; Ward, T. C.; Glasser, W. G. *J. Appl. Polym. Sci.* **1990**, *41*, 2813−2828.
(28) Lewis, R. J. *Hawley's Condensed Chemical Dictionary*, 15th ed.; John Wiley & Sons: Chichester, England, 2007; p 616.
(29) Lederer, M. O.; Klaiber, R. G. *Bioorg. Med. Chem.* **1999**, *7*, 2499−2507.
(30) Eldred, N. R.; Spicer, J. C. *Tappi* **1963**, *46*, 608−612.
(31) Krochta, J. M.; De-Mulder, C. L. C. *Food Technol.* **1997**, *51*, 61−74.
(32) Salame, M. In *The Wiley Encyclopedia of Packaging Technology*, 1st ed.; Bakker, M., Ed.; John Wiley & Sons, Inc: New York, 1986; pp 48−54.
(33) DeLassus, P. T. In *Kirk-Othmer Encyclopedia of Chemical Technolology*; John Wiley & Sons, Inc.: New York, 2002.
(34) Miller, K. S.; Krochta, J. M. *Trends Food Sci. Technol.* **1997**, *8*, 228−237.
(35) Emandi, A.; Vasiliu, C. I.; Budrugeac, P.; Stamatin, I. *Cellul. Chem. Technol.* **2011**, *45*, 579−584.